27 pp.

N63-10889

CODE 1

Technical Report No. 32-329

An Electromagnetic Flowmeter for Low Conductivity Fluids

Niels R. Balling

Benjamin V. Connor

jpl

JET PROPULSION LABORATORY

CALIFORNIA INSTITUTE OF TECHNOLOGY

PASADENA, CALIFORNIA

August 30, 1962

PRICES SUBJECT TO CHANGE

Technical Report No. 32-329

An Electromagnetic Flowmeter for Low Conductivity Fluids

Niels R. Balling

Benjamin V. Connor

D. R. Bartz, Chief
Propulsion Research Section

JET PROPULSION LABORATORY
CALIFORNIA INSTITUTE OF TECHNOLOGY
PASADENA, CALIFORNIA

August 30, 1962

CONTENTS

TABLES

FIGURES

ABSTRACT

/෦‸‸

The measurements of the flow of salt water, tap water, distilled water and n-propyl alcohol by a simply constructed, permanent-magnet flowmeter and associated electronic circuitry are reported. The electromagnetic flowmeter (EMFM) described was developed for measuring the fluctuations in mass-flow rate associated with the study of transient hydraulic phenomena. The system is capable of monitoring fluid-flow fluctuations in the frequency range from 0 cps (steady state) to an estimated maximum frequency of 10 kc. The flow sensitivity, i.e., increment in output amplified voltage across the electrode per increment in fluid-flow velocity, is virtually independent of the fluid conductivity ($\simeq 0.05$ mv/cm/sec) over a range of 0.2 to 5×10^{-8} mho/cm. The potential difference developed across the flowmeter electrodes was measured for fluid velocities ranging from about 2 to 1500 cm/sec. For fluid velocities below approximately 600 cm/sec the observed potential difference followed theory, but above this velocity deviations from theory were apparent. Included are magnetic-field measurements along directions normal to the centerline of the magnetic-pole faces.

I. INTRODUCTION

An experimental project to determine the frequency response of simple rocket-propellant hydraulic feed systems was undertaken at the Jet Propulsion Laboratory. The frequency response of the feed system is represented mathematically by a complex quantity dependent on the applied frequency; its magnitude may be defined as the ratio of the variations in mass flow to the sinusoidal variation in pressure acting on the feed system. Associated with this project is the problem of measuring the fluctuations in mass-flow rate at particular positions in the feed system. The frequencies normally encountered in such investigations range from several cycles to several kilocycles per second. A flow transducer capable of measuring high-frequency fluctuations in velocity, as well as one which, in itself, will not radically change feed-system characteristics, is required. The electromagnetic flowmeter, depending upon the Faraday effect, possesses these characteristics.

The application of the electromagnetic induction method to the measurement of mean velocity in steady and transient flows has been reported in the open literature. The reports utilized during the preliminary phases of this study are presented in the bibliography. None of the reported investigations covered all the desired requirements of (1) range of fluid conductivity, (2) flowmeter sensitivity, and (3) frequency response.

This investigation was directed primarily at the development of a flow-velocity meter to meet the requirement of the project mentioned above, and endeavors to define experimentally the relationship between the generated voltage of the flowmeter as a function of the cross-sectional mean velocity for the range of these parameters of interest.

This Report presents the measurements of the flow of several fluids with conductivities ranging from 0.2 to 5×10^{-8} mho/cm. This range of conductivities is comparable to those associated with the fluids to be used in the feed-system studies mentioned. The fluids used in the test series were salt water (with 30% by weight addition of salt), tap water, distilled water, and n-propyl alcohol. Detection of an ac-component velocity as low as 1 cm/sec was established as a goal.

In conjunction with this work, the transverse magnetic field was measured normal to the centerline of the magnetic pole faces and in a plane containing the flowmeter axis. The conductivities of the fluids were measured before and after the flowmeter calibrations to determine whether or not the amount of contamination acquired during the tests would change significantly the conductivity of the fluid. Other information reported concerns the description of the electronics and associated circuitry as well as the equipment and methods used to make the required measurements. The pressure drop across the flowmeter is given for tap water.

II. FLOWMETER DESIGN

The preliminary considerations involved in the design of the flowmeter were that it should (a) respond to mass-flow rate fluctuations of at least 10 kc/sec, (b) be operable over a range of fluid conductivities from 0.2 to 5×10^{-8} mho/cm, (c) not radically change feed-system characteristics, (d) measure only the alternating component of the mass-flow rate, and (e) have a signal-to-noise ratio that is high enough to detect an ac component of velocity on the order of 1 cm/sec.

During this investigation, two types of EMFM were constructed and tested with two lengths of magnetic field; one with a straight lucite tube as the non-conducting wall, and the other in which the lucite was pressed into a stainless-steel tube. In the latter case, the inner tube can be fabricated easily with either plastic or ceramic liners to provide the non-conducting wall and to seal the electrodes into place. The magnetic field was provided by a permanent magnet for reasons of steadiness, simplicity, and cost. Figures 1 and 2 show the two types of tubes constructed, with details of fabrication. Figure 3 shows the individual parts comprising the flowmeter minus the tube. Figure 4 shows the flowmeter assembled. Figure 5a is a schematic of the flowmeter design showing all pertinent dimensions, and 5b is a cross-sectional view showing construction details. This flowmeter design was based on the several considerations briefly outlined below.

A viscous electrically conducting fluid is made to flow down a tube (Fig. 6) in the o-z direction through a transverse magnetic field in the o-x direction, generating a potential difference in a direction perpendicular to both flow and field (o-y direction). This potential difference is measured by electrodes placed at opposite ends of the o-y diameter of the tube. The potential difference (V) measured is the result of the induced voltage and the circulating currents and electrical resistance losses in the field. The induced voltage and current distribution depend upon the velocity distribution of the fluid. It has been shown by Kolin (Ref. 1) that when the conditions stated below are satisfied, the potential difference can be expressed by this equation:

$$V = \mu H \, dv \times 10^{-8} \text{ v} \qquad (1)$$

The conditions to be satisfied are: (a) that the tube be of circular cross section, (b) that the fluid velocity at any point be a function of radius alone, (c) that the tube have non-conducting walls, and (d) that the magnetic-field

strength and fluid-velocity distribution shall not vary along the tube.

The voltage output of a practical EMFM does not, in general, obey the simple equation usually used (Eq. 1). Shercliff (Ref. 2) and Murgatroyd (Ref. 3), as well as others, have indicated several sources of deviation from Eq. (1), and have theoretically investigated the variations of the potential difference due to several effects. In this report, only those effects that were directly concerned
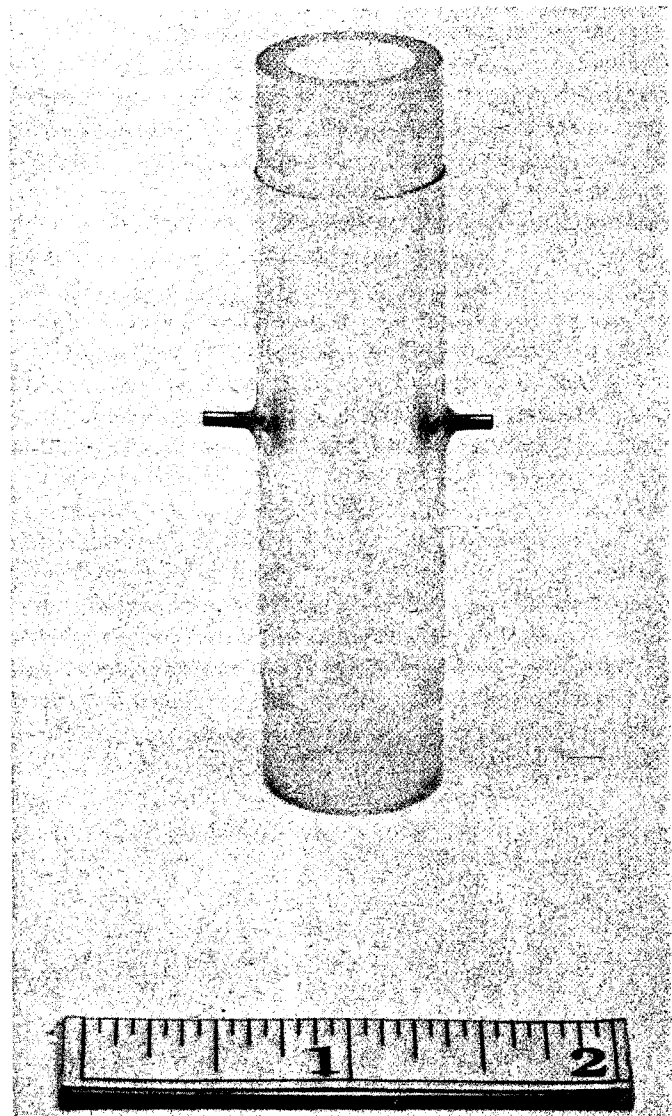

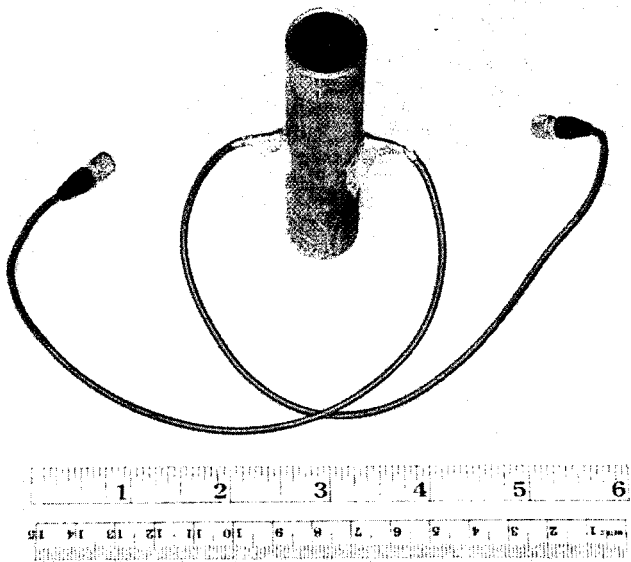**Fig. 1. Lucite flowmeter tube and electrodes**

Fig. 2. Stainless steel flowmeter tube with inner liner of lucite and electrodes

Fig. 3. Flowmeter magnet and component parts

Fig. 4. Flowmeter assembled

cally, variations in the potential difference due to wall conductivity, the shortness of the magnetic-pole faces in the direction of fluid flow, contact resistance of the electrodes, and the difficulties with polarization problems of the electrodes.

Theoretical and experimental results concerning the variation in potential difference due to wall conductivity have appeared where the velocity profile has axial symmetry in circular tubes (Ref. 4, 5). The attenuation of the potential difference due to this effect can be represented by the inclusion of a multiplicative factor appended to Eq. (1); i.e., $V = A_w \mu \, d \, H v \times 10^{-8}$, where

$$A_w = \frac{\left\{\dfrac{2d}{D}\right\}}{\left\{1 + \left(\dfrac{d}{D}\right)^2 + \dfrac{\sigma_w}{\sigma_f}\left[1 - \left(\dfrac{d}{D}\right)^2\right]\right\}} \qquad (2)$$

Equation 2 shows that, for fluids of low conductivity, the wall conductivity must be several orders of magnitude
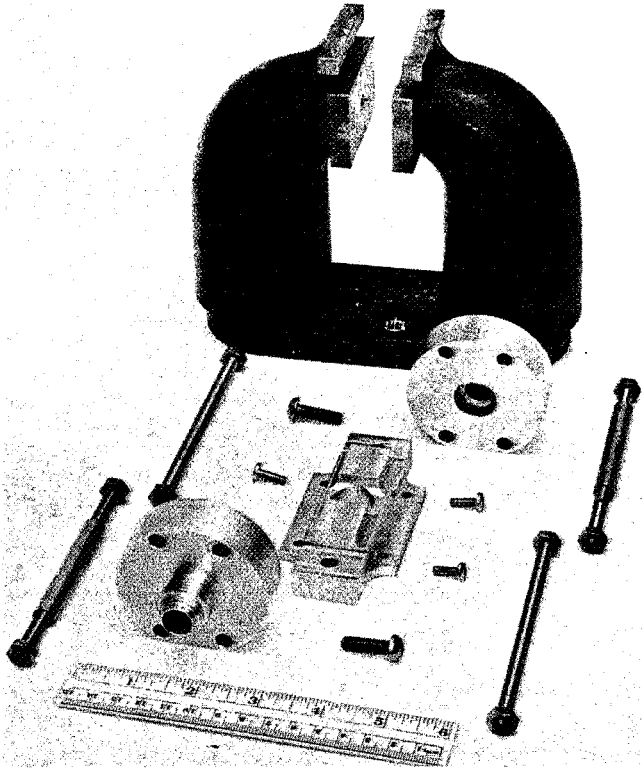
with the design and calibration of the flowmeter investigated will be mentioned. These effects were, specifi-

3

1. PLATINUM ELECTRODES TO BE FLUSH INSIDE TUBE
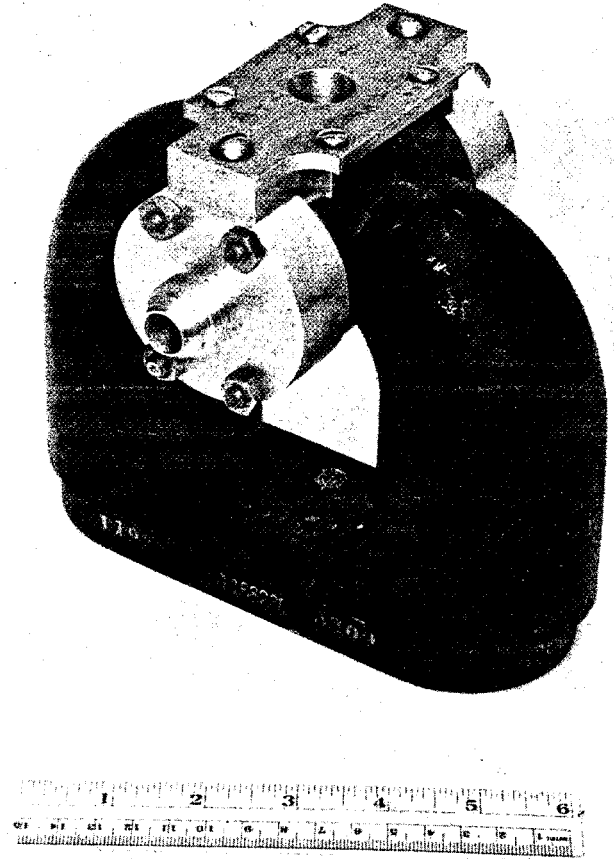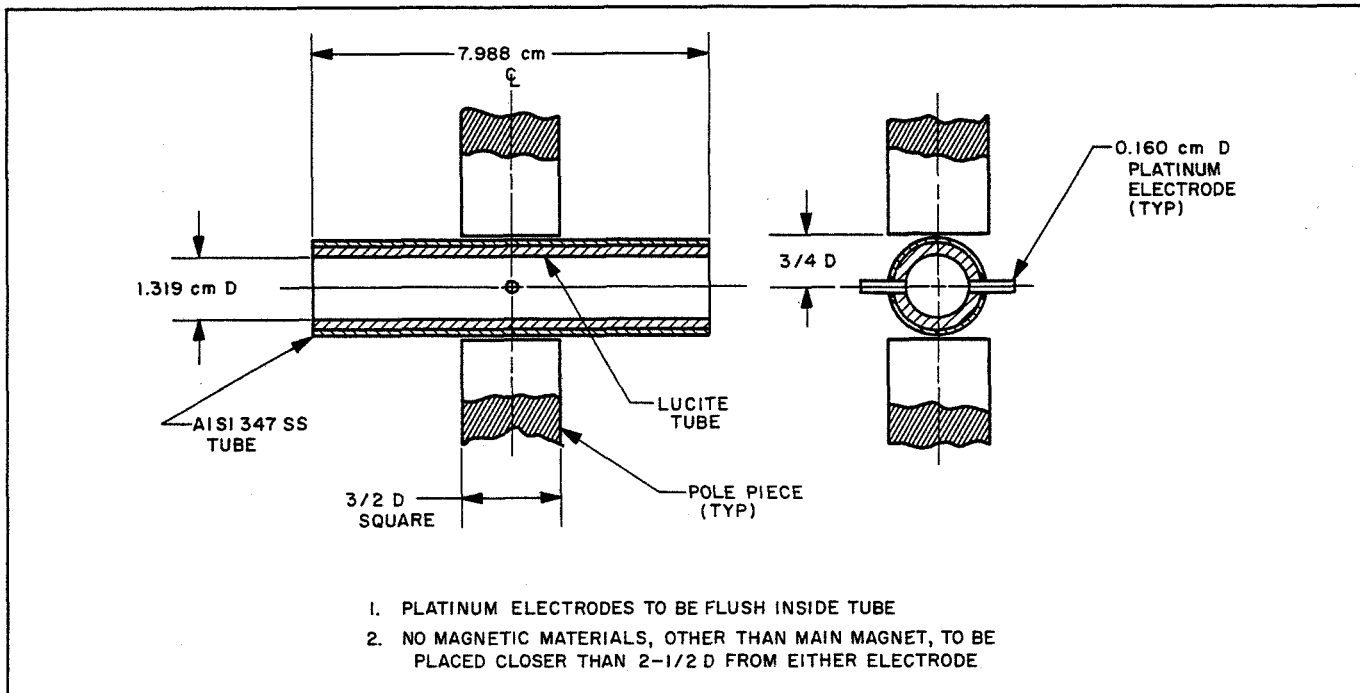2. NO MAGNETIC MATERIALS, OTHER THAN MAIN MAGNET, TO BE
   PLACED CLOSER THAN 2-1/2 D FROM EITHER ELECTRODE

(a) schematic

MATERIAL 6061 T-6 ALUMINUM OR
CRES 347 STEEL
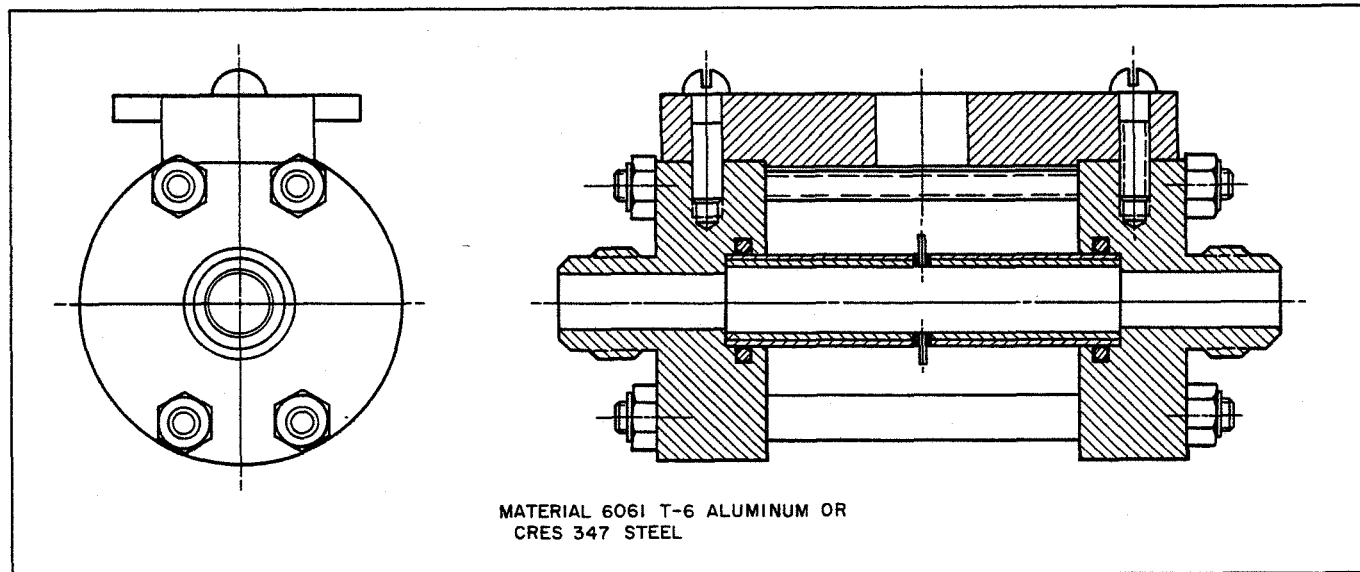
(b) cross section

Fig. 5. Standard electromagnetic flowmeter

lower or appreciable attenuation of the potential differ-ence will be realized. Hence, it was decided to have non-conducting walls in the flowmeter tube and to have the length of the non-conducting tube as large as possible without making the flowmeter configuration unwieldy.

When the pole pieces are short in the direction of fluid flow, secondary currents occur in the flowmeter where the fluid enters and exits the transverse magnetic field. These currents affect the flowmeter potential difference primarily by causing an additional resistance loss, which

is not zero even on the axis of symmetry (Ref. 2). The attenuation factor for this effect (A_H) is applied in the same manner as (A_w) was used to modify Eq. (1):

$$A_H = \left\{ 1 - \frac{8}{\pi^2} \sum_{n_{odd}}^{\infty} \left(\frac{1}{n^2} \right) e^{-n\pi c/d} \right\} \qquad n = 1, 3, 5, \cdots \qquad (3)$$

This attenuation factor was derived, assuming slug flow, constant mean velocity (v), rectangular channel cross section, non-conducting walls, and uniform and parallel magnetic field. Equation (3) shows that $A_H = 0.99$ at $2\,c/d = 2.8$; however, the assumption of an abrupt edge to the magnetic field probably overestimates the attenuation effect. Accordingly, it was decided to measure the potential difference for two different lengths of magnetic field along the flow axis and to compare the measured values with the results predicted by Eq. (3). The lengths of the two pole pieces selected, along the Z axis, were 2.000 and 6.096 cm. The shorter pole-face length was arbitrarily designed to follow as closely as possible the recommended standard flowmeter of Murgatroyd (Ref. 3) consistent with the objectives previously stated. The longer pole face was the maximum practicable length that could be designed into the flowmeter configuration, (Fig. 7a, b and 8).

In regard to the contact resistance of the electrodes, not much information is readily available that is directly applicable to the design. However, an estimate of the relative effect of the contact resistance was made by computing the resistance through a ground of two round plates in parallel planes (Ref. 6). These computations indicated that the smallest surface area of the electrode in contact with the fluid that would not attenuate the

generated flow signal excessively would have a diameter of 1.0 mm or greater. The diameter of the electrode selected was 1.63 mm, because this size wire (14 ga.) was readily available and easily fabricated.

Difficulties associated with electrode polarization have been mentioned (Ref. 1 and 7). These difficulties arise because during operation of the flowmeter the potential difference across the electrodes changes. This potential-difference change disturbs the equilibrium potential of the cell (flowmeter) and a net reaction takes place in the appropriate direction at the electrodes. These reactions are irreversible, the greater the change of potential, the more the current flow, and the greater the irreversibility of the electrode process. An irreversible electrode is said to be "polarized," or to exhibit "overpotential." The polarization or over-potential is caused mainly by three factors: activation polarization, concentration polarization, and ohmic polarization.

Activation polarization is caused by energy being converted to heat when chemical reactions in the cell, caused by the current flow, proceed under non-equilibrium conditions. Concentration polarization is caused when the rate of electrolysis exceeds that at which ions can be brought to the electrodes by migration and agitation; then the electrolyte concentration at the electrode surface falls below the bulk of the solution and ionic transport by diffusion begins. Since the electrodes are now immersed in a region of different concentration from the bulk of the electrolyte, the reversible potential changes. Ohmic polarization depends chiefly on the current flowing in the cell. According to Ohm's law, ohmic polarization is directly proportional to cell current.

Additionally, the electrode reactions will be, for most of the fluids, the cathodic evolution of hydrogen and the anodic evolution of oxygen. These electrode reactions are usually the most irreversible electrode processes encountered in practice. Therefore, the problem was one of determining whether or not the above electrode processes could be minimized in operation with proper circuitry.

Experiments showed that polarizing potentials varied slowly enough to be eliminated by use of capacitive coupling (or other high-pass filtering in the electronics) with cut-off frequencies as low as a few cycles per second. Smooth platinum electrodes gave the least trouble with these spurious variations in the dc-coupled case. These findings checked with those made previously by Laue (Ref. 7). Accordingly, the material selected for the electrodes was platinum, and, except for certain calibration
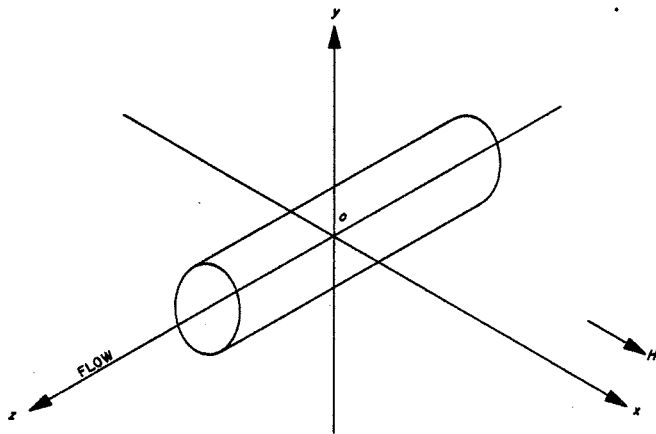
Fig. 6. Schematic showing choice of flowmeter axes

procedures discussed in the next section, capacitive coupling with frequency response down to about 1 cps was used.

An alternative to the dc-coupled system is one in which the magnetic field is alternating. Such a scheme has been used at frequencies as high as 400 cps (Ref. 8), but a flux switching frequency on the order of 100 kc is required for the desired frequency response of 10 kc. Voltages induced across the electrodes by transformer action cannot be entirely eliminated, except by requiring elaborate gating and wave-shaping circuitry to retrieve the signal (Ref. 9). And the electromagnet driver needed to produce the desired "square" flux wave at 50 to 100 kc would require considerable development and would be far from portable.

Fig. 7. Magnetic induction between 2 x 2 cm pole faces: (a) o-z axis; (b) o-y axis

Fig. 8. Magnetic induction between 6.096 x 3.810 cm pole faces, o-z axis

III. TEST APPARATUS AND PROCEDURE

The potential difference generated across the electrodes of the EMFM was experimentally determined as a function of fluid properties and flow conditions. These exp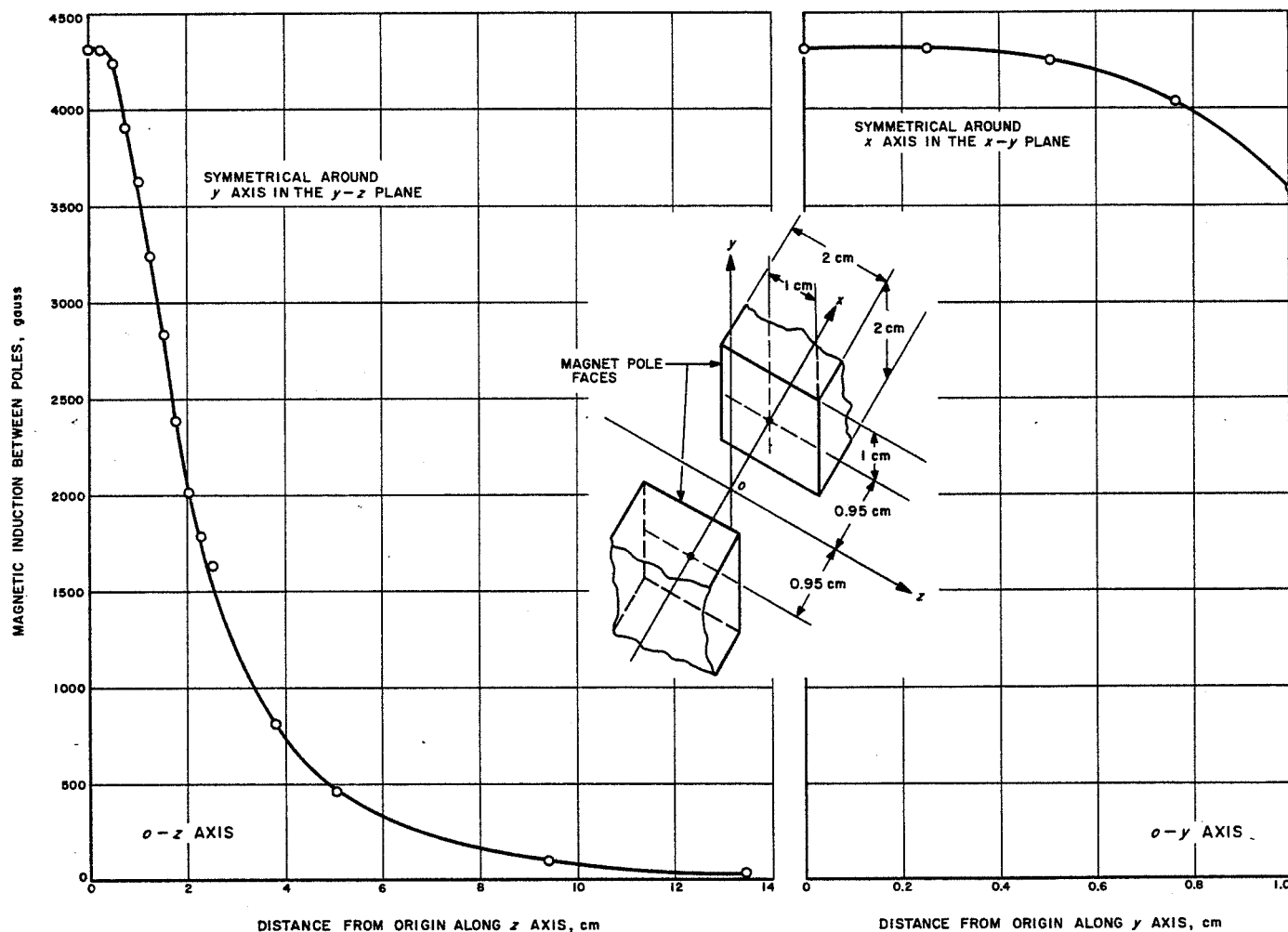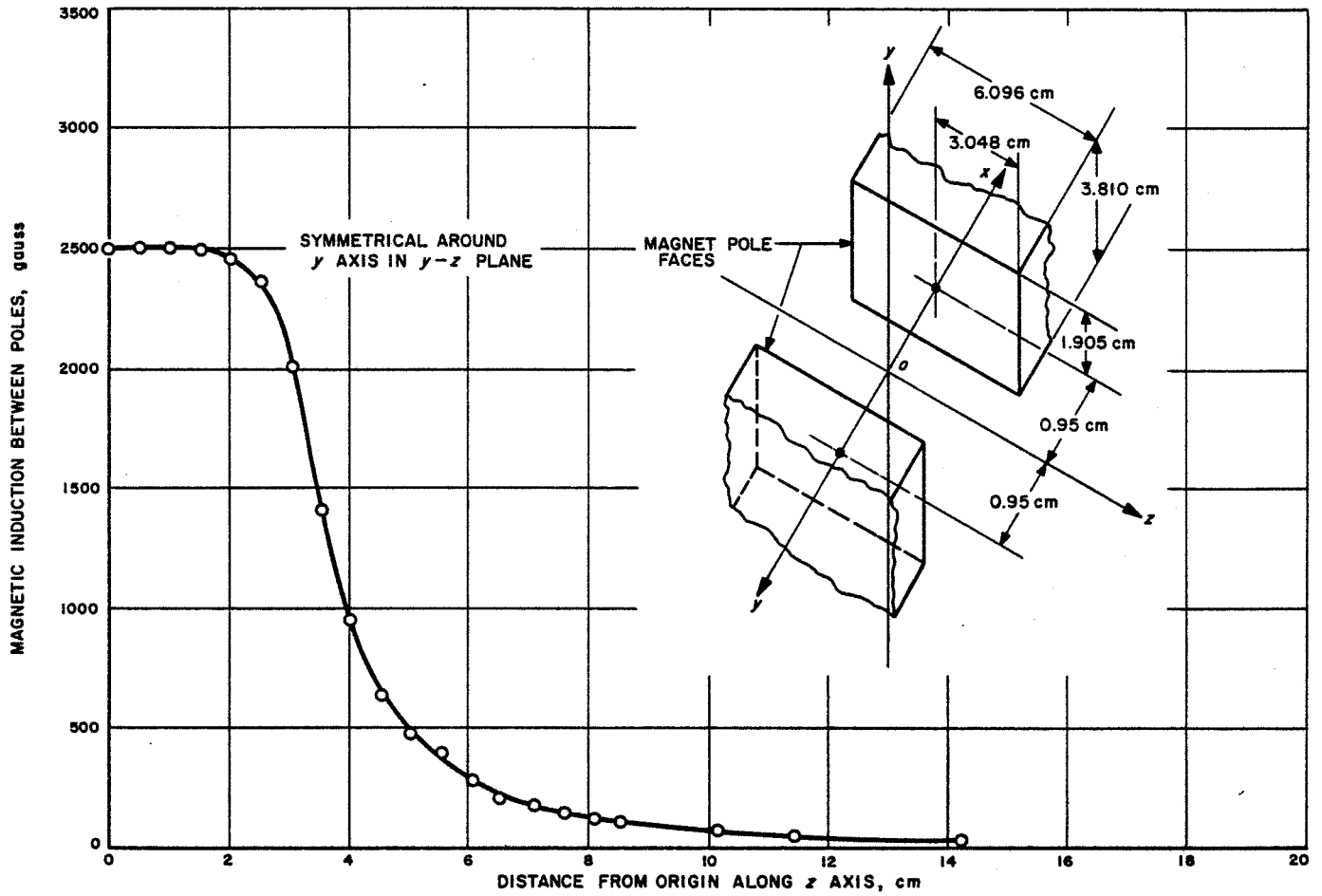eriments can be divided into two categories; those concerned with the evaluation of the steady-state (non-time dependent) characteristics of the device, and those dealing with the response of the meter to dynamic (time dependent) flow conditions.

A. Steady-State Characteristics

The steady-state characteristics, that is, potential developed across the electrodes of the flowmeter as a function of various steady flow rates, were experimentally determined. The results of these tests are shown in Fig. 9a, b and 10a, b. It was the object of these experiments to compare the theoretical analysis with experiment, in particular with the predicted linearity of the flowmeter output as a function of steady-fluid velocity, flowmeter geometry, and fluid.

Figure 11 represents the apparatus used in these steady-state tests. In this apparatus, the test fluid flowed, under the action of compressed nitrogen, from the vertical tank on the wall through the EMFM, a cavitating venturi, and a shut-off valve to the tank in the foreground. In order to assure that the flow possessed axial symmetry, a straight tube having a length-to-diameter ratio of 40 was used as the entrance to the flowmeter.

In addition to the flowmeter, instrumentation was provided to measure the fluid temperature, the pressure drop across the flowmeter, and the pressure immediately upstream of the cavitating venturi. The steady-state mass-flow rate of the cavitating venturis, as a function of upstream pressure, for each of the fluids used, was determined by weight-tank calibration to within $\pm\frac{1}{2}\%$. The inner diameter of the flowmeter was honed out, to be circular in cross section and uniform over the length of the section, with a diameter of 1.319 cm as determined by a standard precision micrometer.

In order to alleviate polarization effects and nullify the drift rate of the flowmeter amplifier, the output from the flowmeter electrodes was capacitatively coupled to the flowmeter amplifier. Data were taken by opening and closing the flow-control valve roughly twice a second (~100 msec to open or close). This caused the flowmeter

amplifier to yield a positive "spike" with rapid rise time (compared to the decay which persisted for ~½ sec) and a typical exponential-decay characteristic when the valve was opened, followed by a negative spike having the same form when the valve was closed (Fig. 12). In this manner, a series of positive and negative spikes would appear as the output of the flowmeter amplifier. The magnitudes of the peaks of the spikes from the base level were taken as the steady-state output of the flowmeter. The average of ten such cycles was taken as 1 data point. Particular attention was devoted to the calibration of this measurement system to assure that the steady-state value was truly represented by the amplitude of the spike's peaks. Calibration before and after each series of runs was accomplished by using a Rubicon to replace the flowmeter as the input to the amplifier. The output of the Rubicon was alternately switched on and off manually, to yield a "spiked" output from the amplifier.

The accuracy of the cavitating flowmeters under these intermittent flow conditions is believed to be within $\pm 1\%$, provided the flow control valve opens smoothly over more than several characteristic propagation time intervals of the hydraulic circuit (i.e., length of the flow circuit divided by the velocity of propagation of a pressure pulse through the liquid tube system $-$ ~2 msec for this system). This is mandatory so as to maintain a pressure near the equilibrium value upstream of the cavitating venturi and to avoid overpressure effects due to too rapid opening or closing of the flow control valve. For opening or closing times on the order of 5 characteristic time periods, these water-hammer effects were observed to be small. Under these conditions, the cavitating venturi apparently follows its equilibrium-operating characteristics. This was verified by measuring the transient flow rate through the EMFM; a turbine flowmeter and the cavitating venturi connected in series. The results of these tests showed that for valve opening times, which permit the turbine flowmeter to follow the flow rate change ($\geqq 0.2$ sec), all the meters exhibit the same indicated flow rate. These measurements also agree well with the theoretically predicted values for this extremely slow opening (or closing) valve. In fact, the theoretical agreement is valid for valve actuation times which are on the order of a few characteristic propagation-time intervals. For valve opening times faster than this, the flow rate as measured by the EMFM and the cavitating venturi flowmeter did not agree closely.
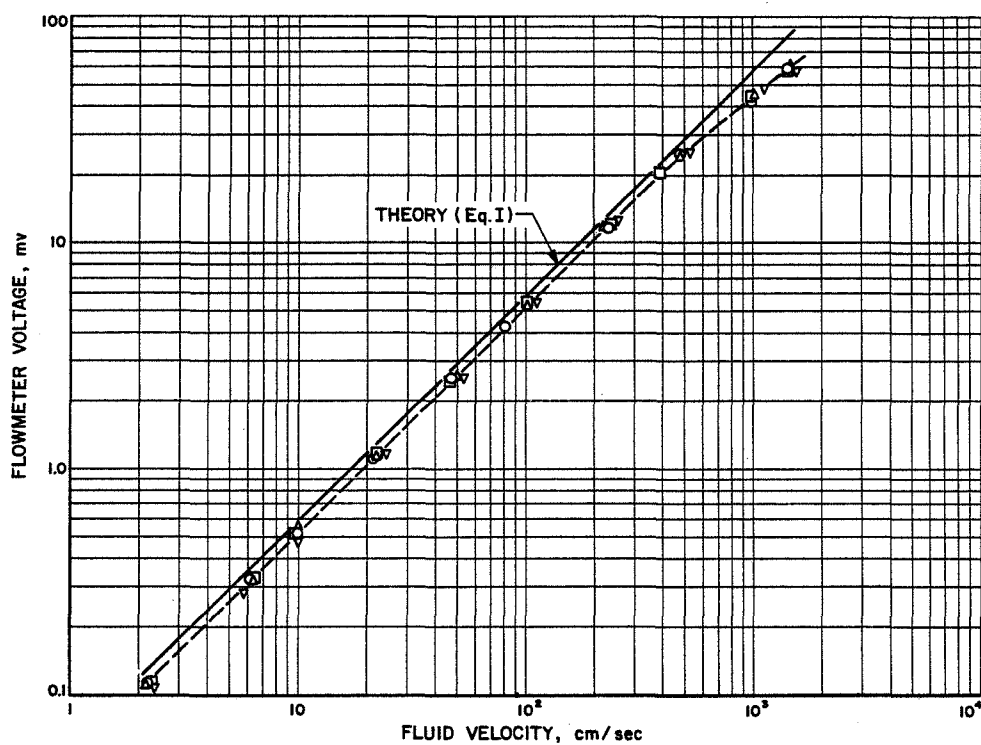
(a) measured potential difference across electrodes
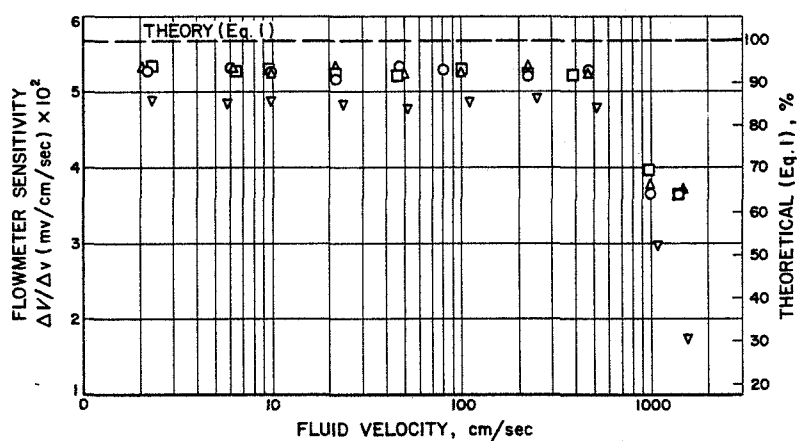
(b) measured sensitivity

SYMBOL	FLUID	σ mho/cm
o	SALT WATER (30% SALT BY wt)	0.2
□	TAP WATER	4.9×10^{-4}
Δ	DISTILLED WATER	$2.8 \times 10^{-6} \rightarrow 1.5 \times 10^{-5}$
▽	n – PROPYL ALCOHOL	5×10^{-8}

Fig. 9. Flowmeter with 2 x 2 cm pole faces
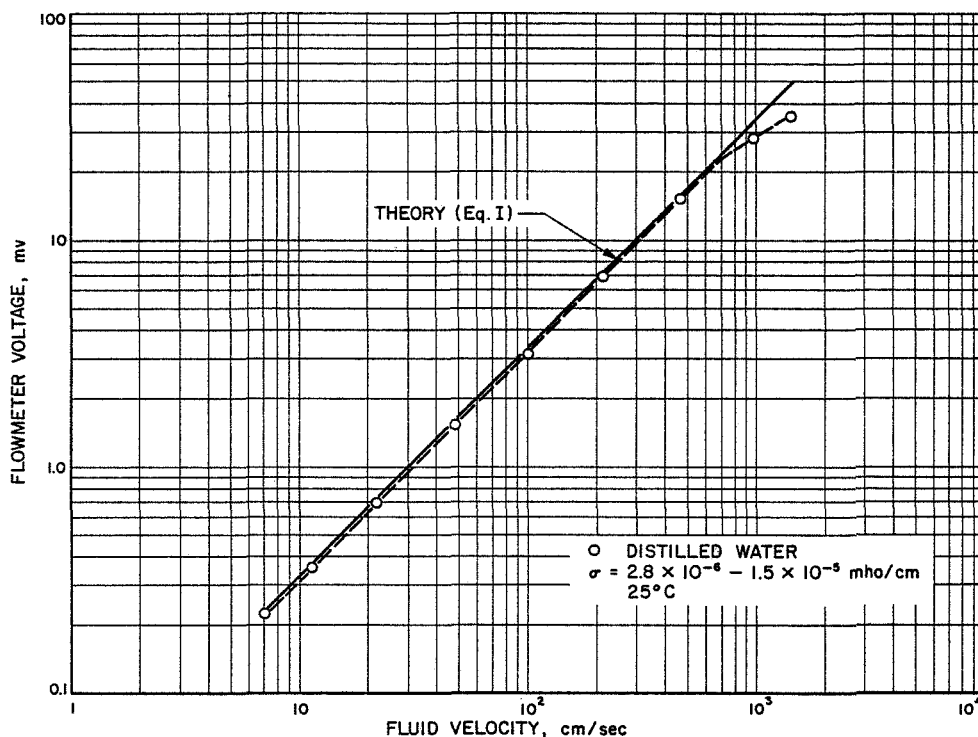
(a) measured potential difference across electrodes
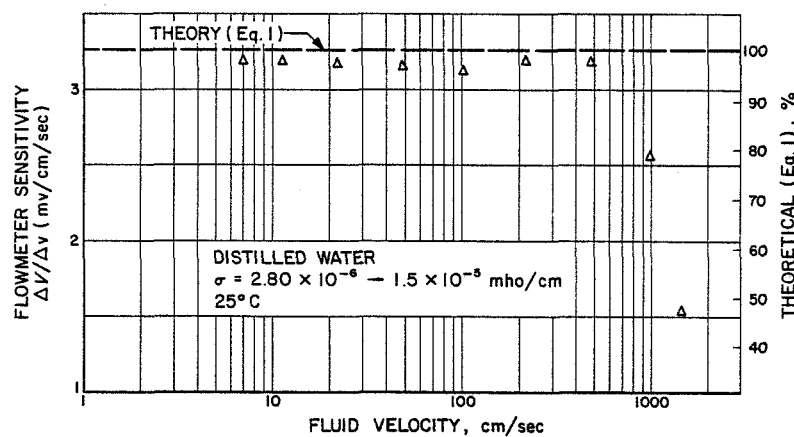
(b) measured sensitivity

Fig. 10. Flowmeter with 6.096 x 3.810 cm pole faces

B. Dynamic Characteristics

The EMFM offers, for the first time, the potential for measuring high-frequency fluid-velocity fluctuations. It was determined that the EMFM produces a potential across its electrodes which is a very good approximation to a linear function of fluid velocity under steady-state conditions (provided the fluid velocity is below ~500 cm/sec, above which point the flowmeter in question exhibited a flow rate, voltage characteristic which was apparently nonlinear). Because of the unavailability of an accurately reproducible source of sinusoidally oscillating flow rate, we can only infer that the dynamic characteristics of the meter (exclusive of the amplifier) will be linear. That is, the flowmeter output amplitude as a function of flowrate at a given frequency will be linear. This paucity of a suitable reference source of sinusoidally-varying flowrate also prevented the determination of

the sinusoidal frequency response; that is, the ratio of observed amplitude and phase of the output to the perturbing amplitude and phase of a sinusoidal-velocity fluctuation at a given flow rate, for various frequencies.

The only apparatus available which could be used as a reproducible, time-varying fluid-velocity source was a water-hammer device. In this device a valve is rapidly closed (in approximately 3 msec) in a line through which liquid is flowing. This causes a shock wave (water-hammer) to propagate upstream where the velocity fluctuations caused by its passage are observed by the EMFM. In this manner, an upper bound on the time constant can be evaluated.[1] From the results of numerous tests it was determined that the rise time of the flowmeter was such that, in all probability, fluid oscillations with frequencies up to $\sim = 10$ kc were faithfully being followed. Therefore, the amplifier frequency response was probably the limiting factor.

This result is in accordance with rise times, observed during the testing of one of these flowmeters, by Iwanicki (Ref. 10), who utilized an aerohydrodynamic shock tube to produce a reproducible step discontinuity in flow velocity. Using this device, rise times were measured on the order of 30 μsec with 10% overshoot corresponding to an estimated frequency response of ~ 15 kc.

C. Testing Precautions

The procedures involved in the use of the electronic equipment are outlined in the discussion of that equipment. A fluid sample for conductivity measurements was taken before the tests and also after a series of tests. This was done to determine whether or not the stainless steel calibration equipment would contaminate the fluid and change its conductivity to an appreciable extent. The magnetic field was measured at the origin before and after each series of tests to make sure that the field strength had not changed (Fig. 7a, b and 8). Between each series of tests, the equipment was thoroughly cleared, and then washed several times with distilled water and allowed to dry completely to avoid contamination of the different fluids.

D. Electronics

The high resistivity of some fluids of interest, the need for non-varying flow calibration with inherent electrochemical effects, and a desire to measure small-flow components over a wide-frequency band, place stringent requirements on the flowmeter amplifier. High input-impedance is necessary to avoid shorting effects, and to hold electrode current, with its associated problems of electrode contamination and polarization voltages, to a minimum. Ideally, the electrodes should see virtually an open circuit for stable operation in this respect. Calculations from measurements using n-propyl alcohol indicate that, for the 1.319 cm diameter flowmeter, the effective flowmeter output resistance is approximately 0.22 times the fluid resistivity; i.e., the reciprocal of the conductivity. This, with the known value of 50 megohms for the amplifier-input resistance, enables us to calculate the relative coupling factor (i.e., loaded flowmeter output/open-circuited output) as a function of fluid resistivity. A plot from the calculations is shown in Fig. 13. Low-signal capability demands low-noise generation and good rejection of spurious signals picked up by the cables.

Since suitable means for absolute dynamic calibration under steady-state periodic-flow conditions (sinusoidal, square wave, etc.) are not available currently, dc-amplifier response is desirable to take advantage of steady-flow techniques of known calibration accuracy.
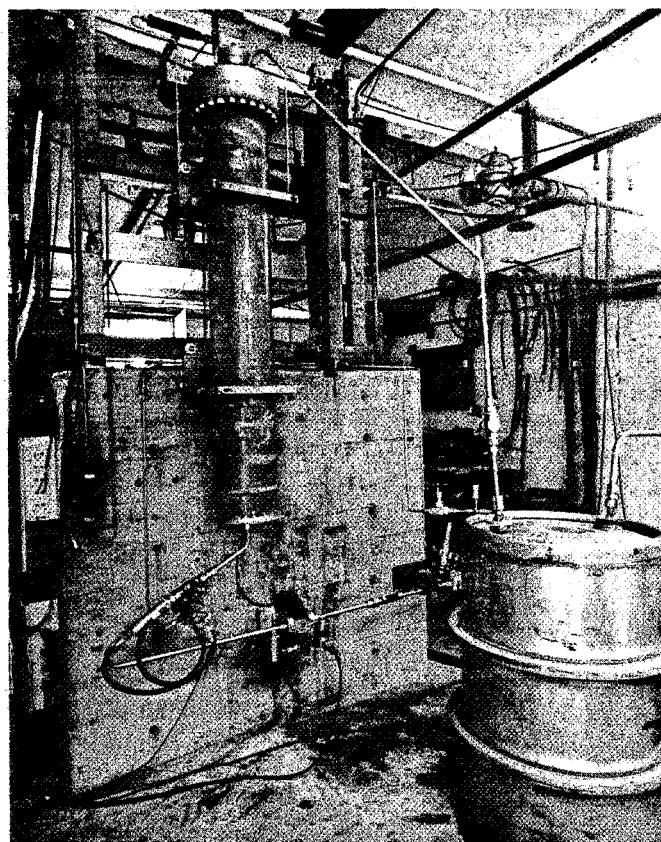

Fig. 11. Flowmeter calibration test setup

---

[1]Characteristic time for the output from the meter to rise to a given fraction $(1 - 1/e) = 0.63$ of its maximum value when perturbed by a step function.
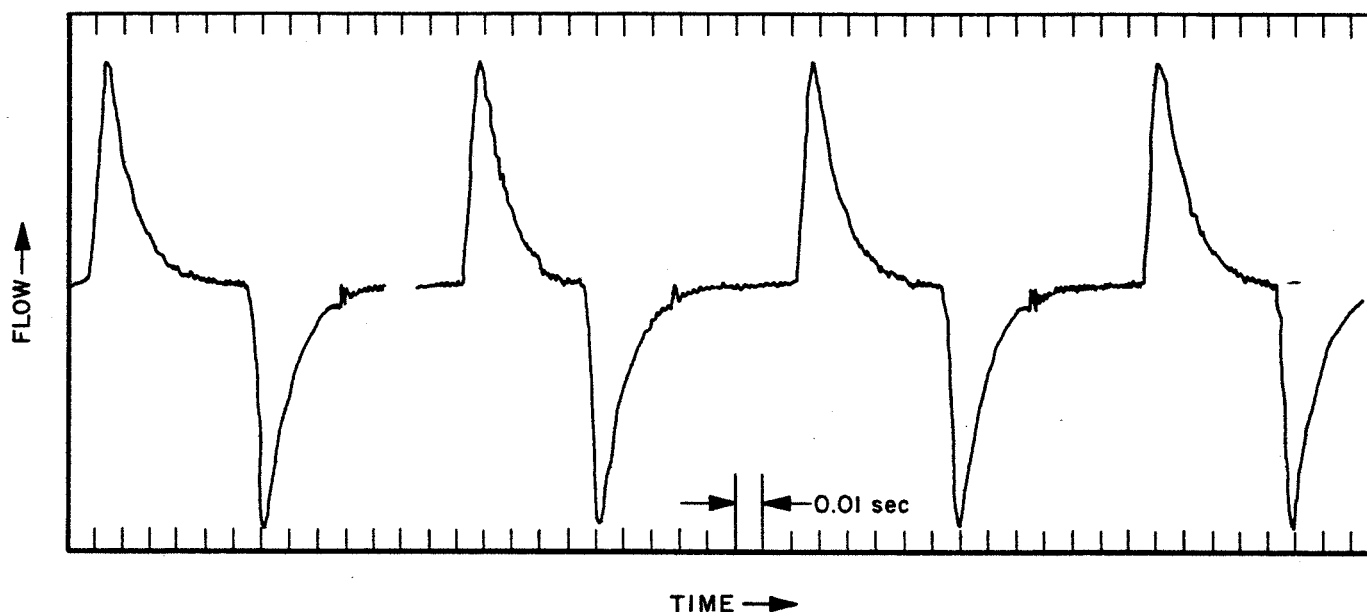
Fig. 12. Oscillograph data sample from typical calibration run

Dynamic response of the amplifier must range to the highest-frequency components expected to exist in the flow during actual operation, and 10 kc was established as the estimated, maximum response requirement. These requirements specify a frequency response that is essentially flat in the range of dc to 10 kc for the amplifier. It is borne in mind that the system-frequency response is affected by the shunting effect of the connecting cable capacitance. For high-fluid resistivity and long cables between flowmeter and amplifier, techniques for reducing this effect (e.g., driven cable shields) may be necessary in order to attain adequate frequency response.

The basic amplifier design is a refinement of one developed in earlier flowmeter work by E. Laue (Ref. 7). Although the final product proved adequate in most respects, it is believed that current advances in the state of the art justify further work concerning the attainment of higher input impedance and lower dc drift.[2] The amplifier circuit is shown in Fig. 14. The differentially-coupled cathode-follower input has an input impedance at dc of 50 megohms and the amplifier has a nominal voltage gain of 3.7, which is flat to 10 kc. The single-ended cathode-follower output will drive a load of 10 kΩ with a loss in gain of less than 1 db. Random noise has been held to less than 25 μv peak-to-peak, referred to the input, which is equivalent to a flow velocity of

approximately 0.5 cm/sec. Dc-output drift after warm-up is unidirectional at ~800 μv/min, which, at the lowest flow rate measured (~2.5 cm/sec), corresponds to an equivalent drift of 2.9% of output signal per second. This drift rate is acceptable in view of the rapidity with which successive calibration steps can be applied and the fact that during routine operation usually only the ac component is of interest, and therefore allows capacity coupling to the amplifier or recorder being driven. Most of this steady drift can be attributed to gradual decline of the battery power-supply voltages; however, the improvements made regarding random fluctuations and 60-cycle hum voltages more than offset this problem.

Various power-supply designs were tried, but severe power-line fluctuations rendered them inadequate regardless of the amount of voltage regulation applied. The ready solution adopted was use of "B" batteries, which was possible because of the relatively low power drain imposed by the amplifier. To further eliminate random drift, a regulated dc-filament supply and special zero temperature-coefficient resistors were adopted which produced a very noticeable improvement. Random high-frequency noise was held to a minimum by selection of low-noise tubes, adjustment of grid bias for best stability in the voltage-gain stage, and a 10 kc low-pass filter in the output for restricting the band-width. Sixty-cycle hum was entirely negligible, being eliminated by the "B" battery approach and good common-mode rejection in the differential input.

---

[2]Along these lines an amplifier having a cathode-follower input circuit with 10[14] ohms input impedance may soon be available and would materially improve the system.
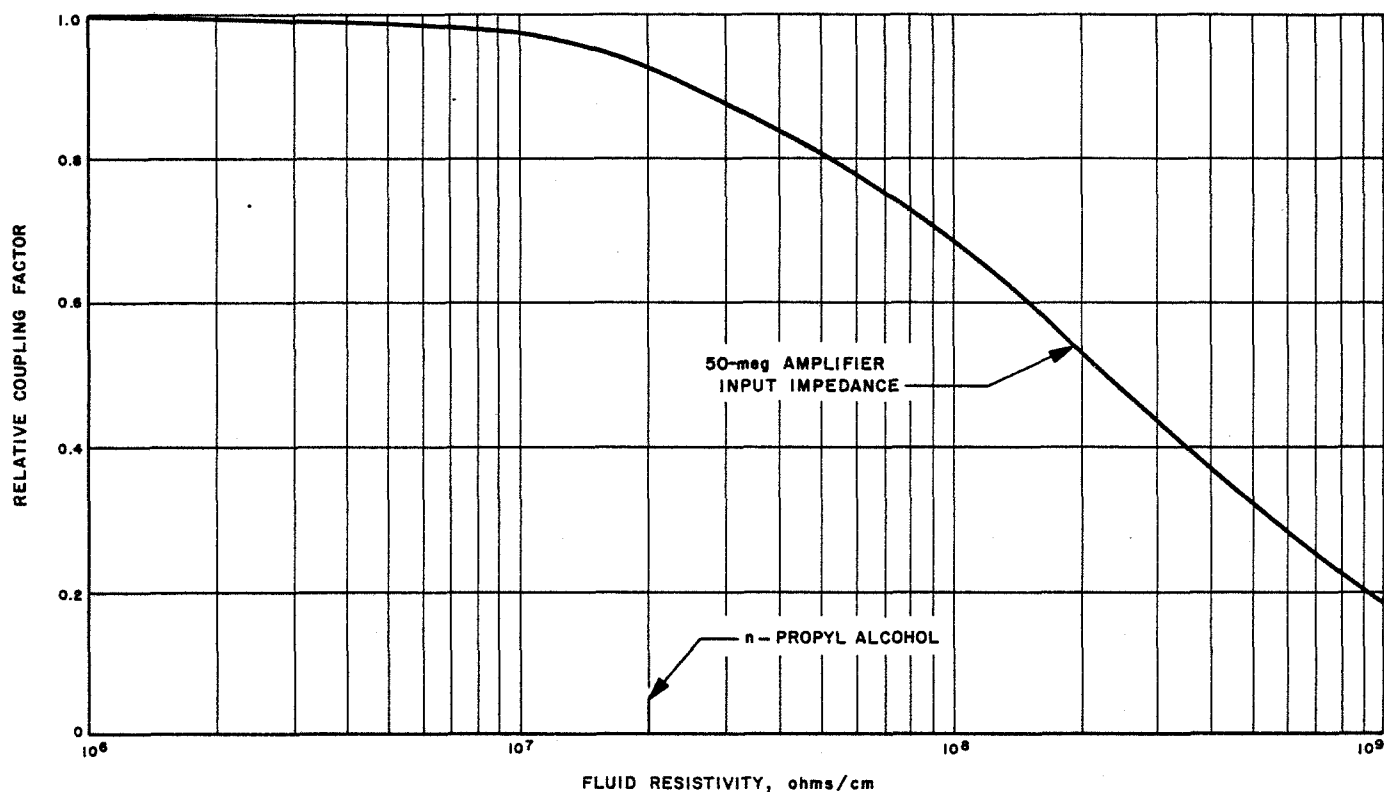
Fig. 13. Relative coupling factor vs. fluid resistivity

The grid potential of the two input cathode-followers, with respect to ground, can be adjusted separately by means of the cathode-voltage adjustments provided (Fig. 12). This provision allows the dc balancing of the input stage, necessary because of unequal, constant electrochemical potentials found existing between each flowmeter electrode and flowmeter case. Under no-flow conditions with tap water, these constant electrochemical potentials amounted to as much as 200 mv, with 20 to 50 mv difference between electrodes. And it was found that some instability or drift was present that could be minimized by placing a bias on the electrodes by means of the cathode adjustments. This problem is discussed (Ref. 7) where this drift and where the bias potentials which give minimum drift are shown to change with time of electrode immersion and to be most stable when platinum electrodes are used. The output cathode-follower can be set to zero dc potential by means of the potentiometer in the cathode of the preceding voltage gain stage.

The flowmeter application determined the types of recording techniques used. For dc calibration, the flow-meter amplifier operates through a voltage divider into a Speedomax or similar device (Fig. 15). For simulated rocket-feed-system runs, and for dynamic calibration where the ac component is of interest, the flow meter amplifier is capacitively coupled to a suitable interme-diate amplifier which, in turn, drives a cathode-ray oscil-loscope or galvanometer oscillograph (Fig. 16). A typical, capacity-coupled calibration sample from the galvanom-eter oscillograph is shown in Fig. 12.

To facilitate correlation of theoretical calculations of sensitivity with measured values, and to compare results obtained with different field configurations, flux distri-butions for two pole-piece shapes were measured with a FE 409-X flux meter for the Alnico V radar magnet used in these investigations. Plots of flux density along the horizontal centerline midway between poles are given in Fig. 7a and 8 and for the two pole pieces investigated, and the results are tabulated in Tables 1 and 3. A plot along the vertical centerline for the 2 x 2 cm pole faces is given in Fig. 7b and tabulated in Table 2. As would be expected, the maximum flux-density value for the 6.096 x 3.810 cm pole faces closely approaches the effec-tive value obtained from comparison of calibrated and calculated sensitivities (Eq. 1), since the field is relatively uniform over the insulation length of the flowmeter. The actual measured sensitivity of the 2 x 2 cm pole pieces,
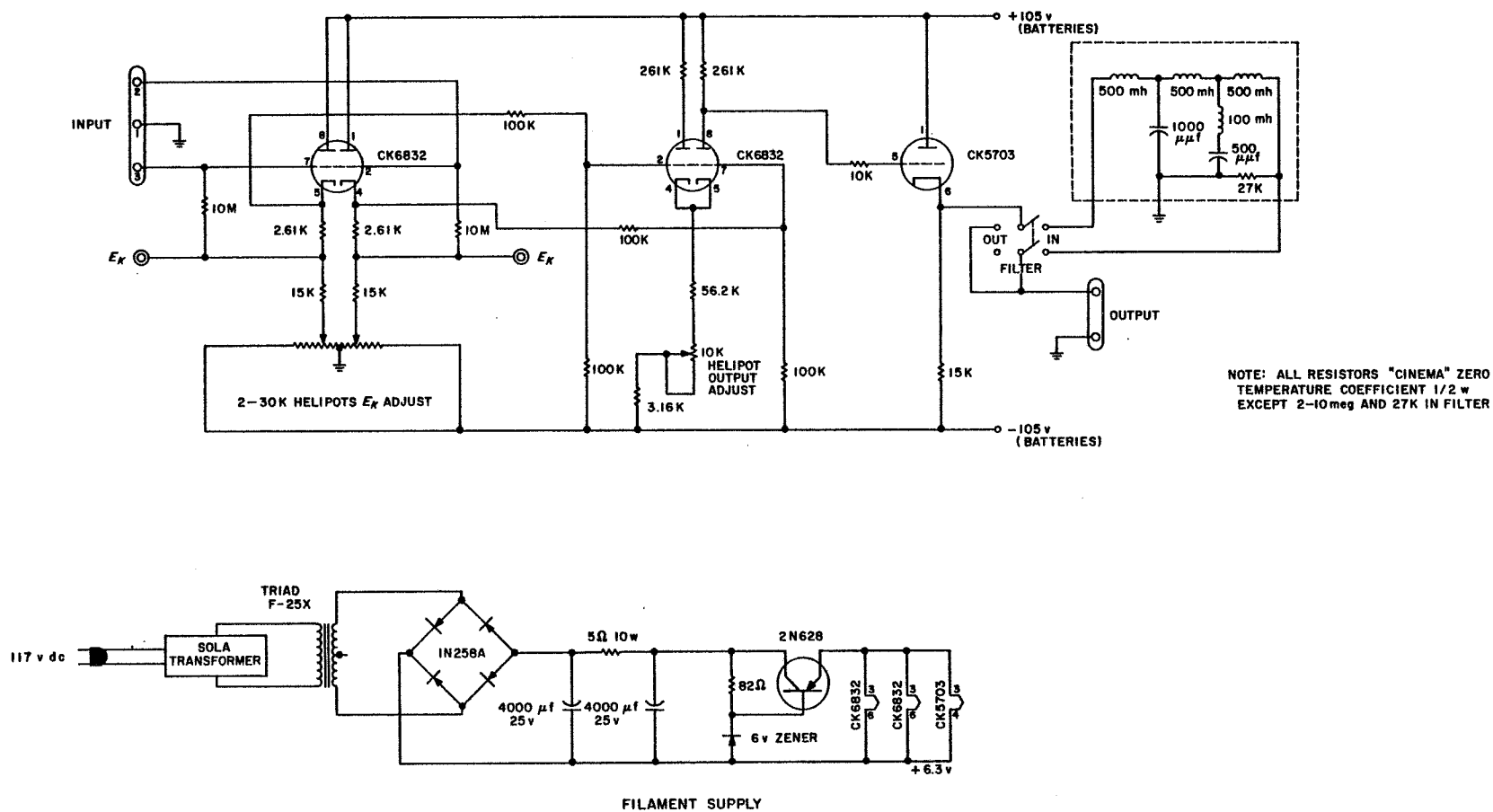
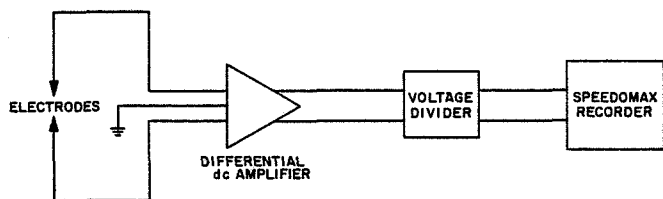**Fig. 14. Flowmeter amplifier circuit diagram**

Fig. 15. Dc calibration circuit block diagram

Fig. 16. Circuit block diagram for ac operation

however, is higher, because the increase in flux density more than offsets a larger difference between maximum and effective values. The estimated maximum error in flux measurement is ±5%.

Conductivity measurements were made using a convenient method developed by Wait (Ref. 11), which allows use of a common pyrex beaker to hold the specimen. A lid for the beaker, made of insulating material, carries four electrodes. Two of them touch the liquid surface diametrically opposed at the beaker walls, across which a voltage is impressed, and two of them touch the surface on the same diameter, spaced one beaker radius apart and centered about the cylindrical axis. Current
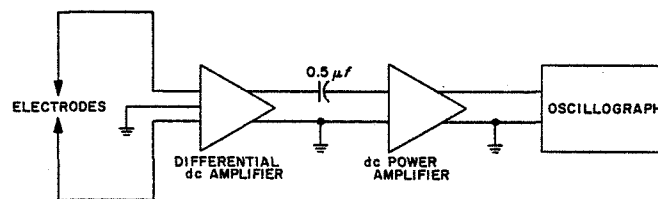
through the outer electrode circuit is measured, and the potential drop across the two inner electrodes is determined by use of an electrometer or other high-impedance voltmeter. The equations for conductivity in terms of the impressed current I and the potential difference between inner electrodes V are derived (Ref. 11) for two ratios of fluid depth to beaker radius, as follows:

$$\frac{V}{I} = \frac{1.0207}{\sigma a} \text{ for } \frac{c}{a} = 1$$

$$\frac{V}{I} = \frac{0.9487}{\sigma a} \text{ for } \frac{c}{a} = 2$$

IV. TEST RESULTS AND DISCUSSION

The calibration results for the flowmeters and various fluids tested are presented in Fig. 9a and 10a as potential difference (V) vs. fluid velocity (v), and in Fig. 9b and 10b as sensitivity, defined as $\Delta V/\Delta v$, vs. fluid velocity (v), for the two pole faces tested; viz., 2×2 and 6.096×3.810 cm. The data used in these figures are tabulated in Table 4. Care was taken in the calibration to obtain points both in the laminar and turbulent flow regions, to test the linearity between the potential difference and the fluid velocity as predicted by Eq. (1). The Reynolds number varied from 30 to 200,000 as the fluid velocity was varied from about 2 to 1500 cm/sec.

Each of the data points shown in Table 4 and Fig. 10a, b represents the mean measured value of a minimum of ten runs. In general, for fluid velocities around 2 or 3 cm/sec, the data exhibited ~10% spread about the mean. This spread rapidly decreased with increasing fluid veloc-

ity, being reduced to ~3% at 40 cm/sec, and at the highest velocities attained, namely, 1500 cm/sec, ~1% spread was measured. For the fluids tested, Fig. 9a, b and 10a, b show that the calibration curve is linear and independent of velocity profile, fluid conductivity, viscosity, and density for fluid velocities from ~2 to ~500 cm/sec. The greater attenuation of the potential difference measured for n-propyl alcohol of ~87% of theoretical, as compared to 92% for salt, tap and distilled water, is due to the shunting effect of the amplifier because its input impedance of 50 meg is too low for a fluid having a conductivity in the range of 10^{-8} mho/cm (Fig. 13).

For fluid velocities of 500 cm/sec, and higher, the calibration deviates significantly from that predicted. As a matter of interest, this effect has been observed on all flowmeters fabricated and calibrated during this investigation; meter sizes ranged from 0.45 to 2.3 cm inner

diameter, using tap water. The abrupt calibration slope change occurs at an electrode current density of ~2.6 x 10⁻⁸ amp/cm² of electrode. This was observed to occur not only with the 1.63 mm diameter platinum electrodes, but also when 1.0 mm platinum electrodes were used.

It is difficult to assign causes for the differences that exist between theory and experiment, because of the several measurements entering into the comparison. The comparison is made, however, taking the various measurements as correct. Under these conditions, the voltage generated by the flowmeter with the 2 x 2 cm pole faces is ~92% of the voltage predicted by Eq. (1) and 137% of that predicted by Eq. (3), the fluid velocities less ~500 cm/sec. The half length of the uniform field was taken as c = 0.50 cm; therefore, 2 c/d = 0.758. The values of the voltage generated using the 6.096 x 3.810 cm pole faces were ~97% of that predicted by Eq. (1) and ~96% of that predicted in Eq. (3), (the half length of the uniform field being taken as c = 2.60 cm, 2 c/d = 3.94). These comparisons show good agreement with both Eq. (2) and (3), for the flowmeter having the long length (6.096 cm) pole faces; however, for the short length (2.00 cm) pole faces, the agreement is not very accurate for either Eq. (1) or (3); Eq. (3) shows a very pessimistic value.

The pressure drop across the flowmeter is presented in Fig. 17. It is shown (Ref. 12) that the pressure drop resulting from magnetic effects should be a linear function of the fluid velocity. For a velocity of 10^2 cm/sec, this effect is calculated to be approximately 2 orders or magnitude lower than that measured. Moreover, from the data presented, the pressure drop across the flowmeter is calculated to be proportional to the fluid velocity raised to the
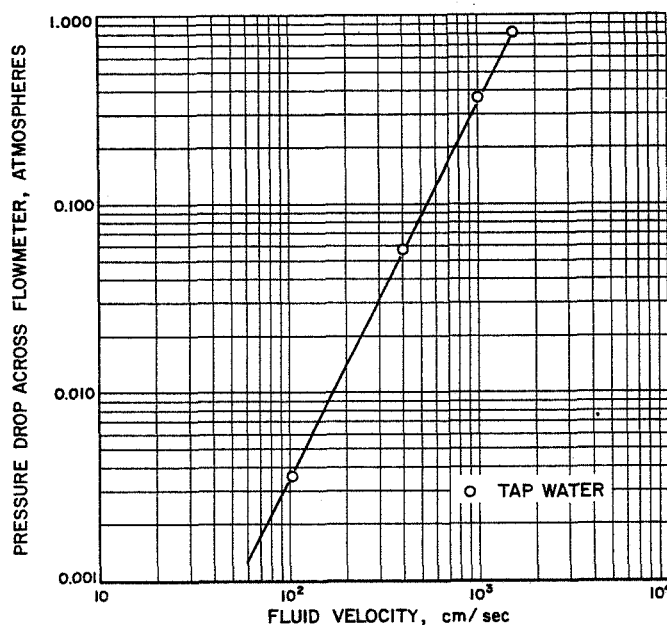

Fig. 17. Pressure drop across flowmeter

1.98 power. From this, one can conclude that the magnetic pressure drop is negligible in comparison with the frictional pressure drop of the flowmeter.

Measurement of fluid conductivity for the test fluids are given in Fig. 9. No measurable contamination was exhibited during the tests with n-propyl alcohol, and, of course, salt water and tap water have such high relative conductivities that the change due to test contamination was also found negligible. Distilled water picked up enough impurities during tests to show a five-fold increase in conductivity, ostensibly, salts, which were more soluble in water than in the higher alcohols.

V. CONCLUSIONS

The experiments performed with the various fluids achieved the stated objectives, with the exception of the required sensitivity which was limited by amplifier noise. The observed noise level of the amplifier was found to be 10% of the signal for the lowest flow rates measured (~2.5 cm/sec), suggesting that the desired 1 cm/sec flow change could not be detected with an acceptably low error. This type of flowmeter has been used successfully for over a year to measure the fluctuating mass flows of simulated rocket-motor feed systems. In practice, flow oscillations of from several cps to nearly 3 kc/sec have been observed. The reproducibility of these measurements has been quite satisfactory.

Table 1. Magnetic induction between pole faces along z-axis* for 2 x 2 cm pole faces

Distance from origin along z-axis, cm	Magnetic induction between poles along z-axis, gauss
0	4321
0.254	4321
0.508	4247
0.762	3919
1.016	3636
1.270	3249
1.524	2831
1.780	2384
2.032	2011
2.290	1788
2.540	1632
3.810	816
5.080	466
9.400	100
13.460	40
*See Fig. 7a.	

Table 2. Magnetic induction between pole faces along y-axis* for 2 x 2 cm pole faces

Distance from origin along y-axis, cm	Magnetic induction between poles along y-axis, gauss
0	4321
0.254	4321
0.508	4253
0.762	4039
1.016	3596
*See Fig. 7b.	

Table 3. Magnetic induction between pole faces along z-axis* for 6.096 x 3.810 cm pole faces

Distance from origin along z-axis, cm	Magnetic induction between poles along z-axis, gauss
0	2503
0.508	2503
1.016	2503
1.524	2496
2.032	2458
2.540	2347
3.050	2012
3.556	1416
4.064	960
4.572	648
5.080	480
5.588	375
6.096	288
6.604	216
7.112	178
7.620	149
8.128	130
8.636	115
10.160	75
11.430	56
14.224	30
*See Fig. 8.	

Table 4. Experimental data for flowmeter calibrations

With 2 x 2 cm pole faces								With 6.096 x 3.810 cm pole faces	
Salt water 30% salt by weight		Tap water		n-propyl alcohol		Distilled water			
Flow velocity v, cm/sec	Potential difference V, mv	Flow velocity v, cm/sec	Potential difference V, mv	Flow velocity v, cm/sec	Potential difference V, mv	Flow velocity v, cm/sec	Potential difference V, mv	Flow velocity v, cm/sec	Potential difference V, mv
2.21	0.117	2.32	0.124	2.35	0.115	2.16	0.115	7.02	0.224
6.05	0.321	6.41	0.338	5.85	0.285	6.18	0.327	11.3	0.361
9.94	0.524	9.72	0.516	10.0	0.487	10.0	0.524	22.0	0.697
21.8	1.13	21.9	1.15	24.3	1.17	21.8	1.16	48.2	1.52
47.2	2.52	45.9	2.40	52.7	2.52	48.5	2.57	101	3.17
80.4	4.26	103	5.46	112	5.47	101	5.32	216	6.91
226	11.8	228	12.0	252	12.4	222	11.8	475	15.1
472	25.1	389	20.3	523	25.1	469	24.5	981	28.1
978	43.6	981	43.8	1100	48.1	987	44.0	1429	35.0
1400	59.0	1400	59.0	1560	56.1	1430	60.3		

NOMENCLATURE

A attenuation of potential difference

a beaker radius, cm

c fluid depth in beaker or half length of uniform magnetic field, cm

d inner diameter flowmeter tube, cm

D outer diameter flowmeter tube, cm

H magnetic induction, gauss

I current, amp

M magnetic number defined as $\mu\, Hd\sqrt{\sigma/\eta}$

n number

v constant or mean fluid velocity, cm/sec

V potential difference

σ fluid conductivity, mho/cm

μ magnetic permeability (taken as unity)

η fluid viscosity

SUBSCRIPTS

f fluid

w wall

REFERENCES

1. Kolin, A., "An Alternating Field Induction Flow Meter of High Sensitivity," *The Review of Scientific Instruments,* Vol. 16, No. 5, pp. 109–116, May 1945.

2. Shercliff, J. A., "The Theory of the D. C. Electromagnetic Flow Meter for Liquid Metals," A.E.R.E. XIR 1052, 1953.

3. Murgatroyd, W., "The Model Testing of Electromagnetic Flow Meter," XIR 1053, 1953.

4. Elrod, H. G. and R. R. Loose, "An Investigation of Electromagnetic Flow Meters," *Transactions of American Society of Mechanical Engineers,* Vol. 74, p. 589, May 1952.

5. Astley, E. R., "Magnetic Flow Meter Output Potentials," *General Electric Report,* No. 52, 6L, p. 42, March 1952.

6. Dwight, H. B., "Calculation of Resistances to Ground," *Transactions of American Institute of Electrical Engineers,* p. 1319, 1936.

7. Laue, E. G., "Application of the Electromagnetic Flow Meter to the Testing of Liquid-Propellant Rocket Motors," *Memorandum No. 20-109,* Jet Propulsion Laboratory, Pasadena, March 1955.

8. Shirer, H. W., R. B. Shackleford, and K. E. Jocim, "A Magnetic Flow Meter for Recording Cardiac Output," *IRE Proceedings,* Vol. 47, No. 11, p. 1901, November 1959.

9. Westersten, A., G. Herrold, E. Abbott, and N. S. Assali, "Gated Sine-Wave Electromagnetic Flowmeter," *IRE Transactions on Medical Electronics,* Vol. ME 6, p. 4, December 1959.

10. Iwanicki, L., "Results of the Electromagnetic Flowmeter Calibration Tests," *Rocketdyne Report,* LER, 1141–4004, May 1961.

11. Wait, R., Jr., "Measurement of Conductivity of a Fluid Contained In a Cylindrical Vessel," *Canadian Journal of Technology,* Vol. 34, p. 410, 1957.

12. Shercliff, J. A., "Steady Motion of Conducting Fluids In Pipes Under Traverse Magnetic Fields," *Proceedings of the Cambridge Philosophical Society,* Vol. 49, p. 136, 1953.

BIBLIOGRAPHY

1. Einhorn, H., *Proceedings of the Royal Society* (South Africa), Vol. 28, p. 143, 1940.

2. Greenhill, M., "Electromagnetic Pumps and Flowmeters," Atomic Energy Research Establishment, Harwell (a bibliography of literature and government reports), 1954.

3. Jaffe, L., B. Coss, and D. F. Daykin, *RM E 50L12*, National Advisory Committee for Aeronautics, March 1951.

4. Kolin, A., "Electromagnetic Velometry I & II," *Journal of Applied Physics*, Vol. 15, pp. 150–164, 1944, and Vol. 25, pp. 409–413, 1954.

5. Morris, A. J., and J. H. Chadwick, *Transactions Conference* Paper T-1-58, American Institute of Electrical Engineers, 1951.

6. Thürlemann, B., *Helvetica Physica Acta*, Vol. 14, p. 383, 1941.

7. Williams, E. J., *Proceedings of the Physical Society* (London), Vol. 42, p. 466, 1930.